JCTC Journal of Chemical Theory and Computation

Molecular Dynamics Simulation Study of the Influence of Cluster Geometry on Formation of C_{60} Fullerene Clusters in Aqueous Solution

Hojin Kim,[†] Dmitry Bedrov,[‡] and Grant D. Smith*[,†,‡]

Departments of Chemical Engineering and Materials Science and Engineering, 122 South Central Campus Drive Room 304, University of Utah, Salt Lake City, Utah 84112

Received August 22, 2007

Abstract: We have performed atomistic molecular dynamics simulations of linear (1-dimensional), planar (2-dimensional), and icosahedral (3-dimensional) clusters of C_{60} fullerenes in aqueous solution in order to investigate the influence of cluster geometry on their free energy of formation. As was found in our previous study of the potential of mean force (PMF) as a function of separation for a single pair of fullerenes in aqueous solution, the interaction between fullerenes for all cluster geometries was dominated by direct fullerene−fullerene interactions and not by water-induced hydrophobic interactions. A coarse-grained implicit solvent (CGIS) potential, given by the PMF for the fullerene pair in water obtained from atomistic simulations, was found to describe well the free energy of formation of the linear cluster, indicating that many-body effects, i.e., the influence of neighboring fullerenes on the water-induced interaction between a fullerene pair, are negligible for the 1-dimensional geometry. For the 2-dimensional and particularly the 3-dimensional geometry, however, many-body effects were found to strongly influence hydration, leading to complete dehydration of the central fullerene at close fullerene−fullerene separations for the icosahedral cluster. This strong influence of geometry on hydration translates into water-induced interactions that, while remaining repulsive, as is found for the fullerene pair, are not well described by the two-body CGIS potential obtained from the isolated fullerene pair, particularly for the 3-dimensional geometry.

I. Introduction

Because of their nonpolar character and extremely low solubility in water, C_{60} fullerenes are often considered to be hydrophobic molecules. However, in recent simulation studies[1,2] we found that the attraction between two fullerenes, given by the potential of mean force (PMF) as a function of their separation, is actually *weaker* in water than in vacuum. Hence, in contrast to hydrophobic particles of the same size (e.g., one nanometer diameter oil droplets), water actually promotes dispersion of the fullerene pair. The favorable water-fullerene interaction is due to the strong van der Waals interactions between the fullerenes and water resulting from the high atomic surface density of fullerene. The strong van der Waals interaction of fullerenes with various gas molecules has also been observed in ab initio and density functional calculations.[3] These favorable interactions overcome loss of hydrogen bonding and entropic restrictions on water at the fullerene surface. Nevertheless, despite the water-induced repulsion, the strong direct van der Waals interactions between two fullerenes dominate the PMF resulting in a strong attractive interaction (−4.2 kcal/mol) for two fullerenes in direct contact.[1] These strong direct fullerene−fullerene van der Waals interactions are the primary reason for the insolubility of fullerenes in water.

From the PMF studies of two fullerenes in water we have derived a coarse-grained implicit solvent (CGIS) potential[1]

* Corresponding author e-mail: gsmith2@cluster2.mse.utah.edu.
[†] Department of Chemical Engineering.
[‡] Department of Materials Science and Engineering.

10.1021/ct700211y CCC: $40.75
Published on Web 01/15/2008

that describes both direct fullerene−fullerene interactions and effective fullerene−fullerene interactions due to water. We have utilized this potential to study the self-assembly of bare and polymer modified C_{60} fullerenes in water.[4] This two-body potential assumes that the free energy of formation of fullerene aggregates (clusters) can be described as the sum of the CGIS potential over all fullerene pairs. However, it can be anticipated that as the fullerene cluster size and dimensionality increase the structure of water hydrating each fullerene pair can depend on the relative position of neighboring fullerenes and therefore the water-induced interactions can be different from those obtained for an isolated pair of fullerenes. In this work, we investigate the free energy of formation of 1-dimensional, 2-dimensional, and 3-dimensional fullerene aggregates in aqueous solution and the applicability of the two-body CGIS potential to these geometries. For this purpose we have performed fully atomistic molecular dynamics (MD) simulations to determine the free energy for formation of the fullerene aggregates. MD simulations are suitable to study a small fullerene cluster and previously have been utilized to investigate the phase behavior of the small fullerene cluster, $(C_{60})_7$, in vacuum.[5,6] Discrepancies between the CGIS and atomistic predictions indicate the existence of a many-body effect in fullerene clusters whose nature is discussed in detail.

II. Methodology

A. Atomistic Simulations. All MD simulations have been carried out using the simulation package *Lucretius*.[7] For atomistic simulations of the fullerene-water solution, interactions were described by a Lennard-Jones potential[8]

$$U_{LJ}(r) = 4\epsilon\left[\left(\frac{\sigma}{r}\right)^{12} - \left(\frac{\sigma}{r}\right)^{6}\right] \quad (1)$$

where r is a distance between atoms, while σ and ϵ are the parameters related to the atomic size and the strength of attraction, respectively. For carbon−carbon interactions the parameters $\sigma_{c-c} = 3.47$ Å and $\epsilon_{c-c} = 0.275$ kJ/mol[1] were utilized. For water, the transferable intermolecular four-point potential (TIP4P)[9] water model was employed, and C_{60}-water interactions were represented by a Lennard-Jones potential ($\sigma_{c-o} = 3.19$ Å and $\epsilon_{c-o} = 0.392$ kJ/mol) which was empirically parametrized to recover the macroscopic contact angle of a water droplet on graphite.[10] All bond lengths were constrained using the SHAKE algorithm,[11] and the C_{60} fullerenes were made completely rigid through addition of additional bonds. The particle mesh Ewald algorithm (PME)[12] was used to handle the long-range water−water Coulomb interactions. Production runs were carried out in the NVT ensemble (constant volume and temperature) using a multiple-time-step reversible reference system propagator algorithm.[13,14] A time step of 0.75 fs was used for nonbonded (Lennard-Jones and real part of Coulomb) interactions within a cut off radius of 7 Å, while a time step of 3 fs was used for nonbonded interactions for separations between 7 and 10 Å and reciprocal part of the Coulomb interactions.

B. Systems Studied. In this study, the fullerene clusters consisted of 3, 7, and 13 C_{60} fullerenes labeled $(C_{60})_3$, $(C_{60})_7$, and $(C_{60})_{13}$, as illustrated in Figure 1. The $(C_{60})_3$ cluster is linear, the $(C_{60})_7$ cluster is close-packed planar, and the $(C_{60})_{13}$ cluster has an icosahedral geometry. In the $(C_{60})_3$ and $(C_{60})_7$ clusters, dummy atoms that do not interact with any other atoms were used to constrain the clusters to linear or planar geometries, respectively. All fullerenes (center-of-mass) were maintained at an equal distance from the center-of-mass of the central fullerene of the cluster with a range of separations of 9.25−17.0 Å at increments in spacing of 0.5 or 0.25 Å, depending upon the separation. All fullerene−fullerene distances in the clusters were constrained by the SHAKE method to maintain both the distance of the fullerenes to the central fullerene as well as the cluster geometry (linear, close-packed planar, or icosahedral).

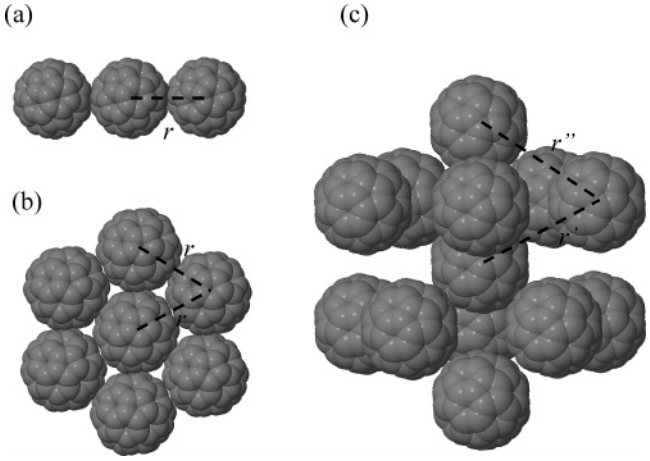

Figure 1. Geometries of the (a) $(C_{60})_3$, (b) $(C_{60})_7$, and (c) $(C_{60})_{13}$ fullerene clusters. r represents the fullerene−fullerene separation distance for clusters (a) and (b) and an average (over all 42 nearest neighbor pairs) of r' and r'' for cluster (c). Here, r' is the separation between shell fullerenes and the central fullerene, and r'' ($r'' = 1.05r'$) is the nearest neighbor shell−shell separation.

Equilibration of the systems, which consisted of a single cluster and 6000 water molecules, to yield equilibrium densities was carried out using a periodic cubic cell in the NPT (constant pressure and temperature) ensemble at 298 K and 1 atm with a separation distance (of all shell fullerenes to the center of the cluster) of 17.0 Å for 500 ps. Following equilibration, NVT simulations were performed at the various separation distances for a sampling time of 5−15 ns. In addition to the clusters, a single fullerene pair, $(C_{60})_2$, was also examined in a cubic cell containing 2000 water molecules using the same simulation protocol.

C. Determination of the Potential of Mean Force. The potential of mean force (PMF) was obtained from integration of the mean constraint force

$$PMF(r) = -n_{shell}\int_r^{r_{max}}\left[<F_{con}(r)> - \frac{2k_BT}{r}\right]dr \quad (2)$$

where r is the separation distance between the center-of-mass position of the shell fullerenes (those surrounding the central fullerene of the cluster) and the center-of-mass of the cluster, $<F_{con}(r)>$, is the mean constraint force experienced by each shell fullerene along the bond connecting it to the central fullerene, and r_{max} is a distance sufficiently

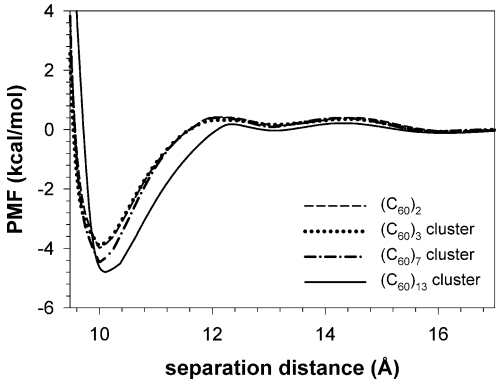

Figure 2. The potential of mean force (PMF) for various fullerene clusters as a function of separation. Each PMF has been normalized by the number of nearest neighbor fullerene pairs in the cluster.

large (17.0 Å) such that $<F_{con}(r)> - 2k_BT/r \approx 0$. The parameter n_{shell} is the number of fullerenes surrounding the central fullerene, with $n_{shell} = 2$, 6, and 12 for the linear, planar, and icosahedral geometries, respectively, and k_B is the Boltzmann constant. Note that by symmetry the only constraint force experienced by a fullerene on average lies along the bond connecting it to the central fullerene. $<F_{con}(r)>$ represents an average over both time and all n_{shell} fullerenes. The quantity $PMF(r)$ is the free energy change associated with bringing the fullerenes of the cluster together to a separation r from the central fullerene (with the correct geometry) from a far separation and hence is referred to as the free energy of formation for the cluster.

III. Results

A. Potential of Mean Force. In order to understand the influence of cluster geometry on the free energy of cluster formation, it is useful to normalize the PMF given by eq 2 by the number of nearest neighbor pairs in the cluster, which is 1 for $(C_{60})_2$, 2 for $(C_{60})_3$, 12 for $(C_{60})_7$, and 42 for $(C_{60})_{13}$. Furthermore, while all nearest neighbor pair separations are equal to the separation r between the shell and central fullerenes for the $(C_{60})_2$, $(C_{60})_3$, and $(C_{60})_7$ clusters, this is not the case for the $(C_{60})_{13}$ cluster. Here, the nearest neighbor distance between shell fullerenes is slightly greater (by 5%) than the separation between shell and central fullerenes as required by the icosahedral geometry. The separation distance r for this cluster for all plots in this paper is an average over all (42) nearest neighbor pairs.

The (normalized by the number of nearest neighbor pairs) PMF as a function of separation is shown for all cluster geometries in Figure 2. All PMFs exhibit one deep minimum at a separation distance of around 10 Å, indicating the van der Waals contact distance for the fullerenes, and oscillatory features at larger separation that reflect the structure of the hydrating water, as discussed previously for the fullerene pair.[2] The shallow minimum at about 13 Å corresponds to a single layer of hydrating water between the fullerenes while that at about 16 Å to two layers of hydrating water. The slight shifting of the contact minimum to larger separation for the $(C_{60})_{13}$ cluster reflects the fact that the distance between nearest neighbor fullerene pairs in the shell is slightly greater than that between the central fullerene and the shell fullerenes.

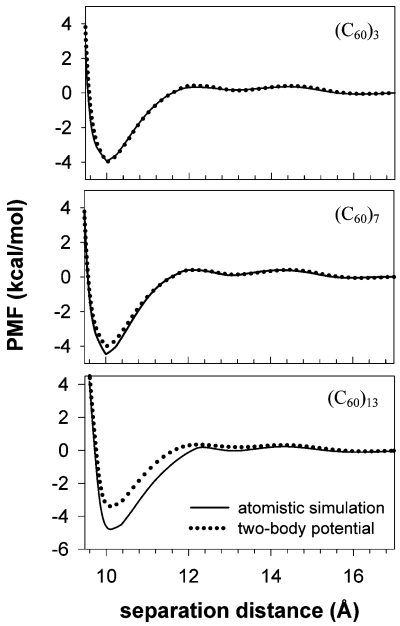

Figure 3. Comparison of the potential of mean force (PMF) obtained from atomistic molecular dynamics simulations and as predicted by the two-body coarse-grained implicit solvent potential.

While all PMFs show qualitatively similar behavior, it is clear from Figure 2 that the free energy of formation depends upon cluster geometry. As the dimension of the cluster increases the depth of the primary minimum increases. Furthermore, the position of the first peak in the PMF for the $(C_{60})_{13}$ cluster is shifted to a larger separation distance than for the 1- and 2-dimensional clusters. This shift is greater than that observed for the contact minimum position, indicating that the shifting reflects not only the difference between shell−shell fullerene and shell-central fullerene separations but also a significant fundamental difference in the effective interactions between the fullerenes of the 3-dimensional cluster compared to the 1- and 2-dimensional aggregates.

B. Comparison with the Coarse-Grained Implicit Solvent Two-Body Potential. Insight into the effect of cluster geometry, and hence into the influence of many-body interactions, on the free energy of formation of fullerene clusters in aqueous solution can be gleaned by comparing the free energy of formation obtained from atomistic simulations with that predicted using the two-body coarse-grained implicit solvent (CGIS) potential. In the CGIS model we assume that the free energy associated with forming nearest neighbor fullerene pairs in each cluster is described (as a function of separation) by the PMF for the $(C_{60})_2$ cluster obtained from atomistic simulations (see Figure 2). The resulting (normalized by the number of nearest neighbor pairs) CGIS PMF for the $(C_{60})_3$, $(C_{60})_7$, and $(C_{60})_{13}$ clusters is compared with that from fully atomistic simulations in Figure 3.

For the $(C_{60})_3$ cluster the PMF obtained from the two-body CGIS model is nearly identical to that obtained from atomistic simulations. In this linear 1-dimensional geometry,

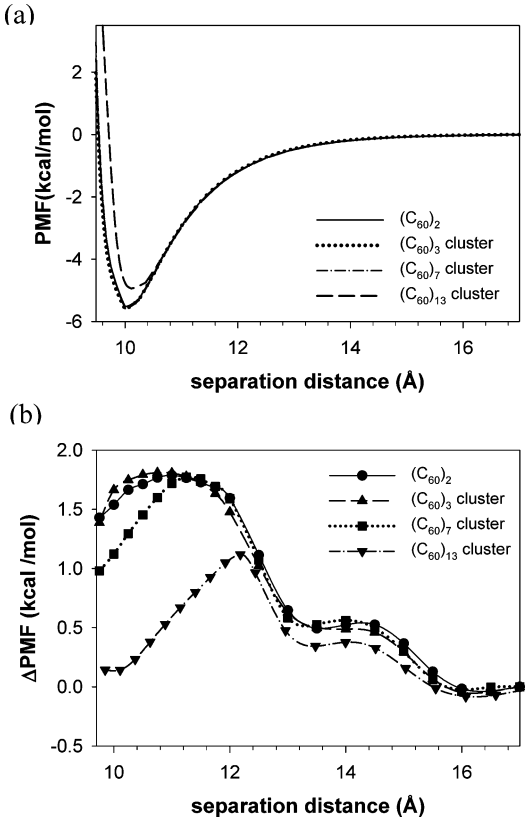

Figure 4. The (a) in vacuo and (b) water-induced contribution to the potential of mean force (PMF) for each cluster geometry. Each PMF has been normalized by the number of nearest neighbor fullerene pairs in the cluster.

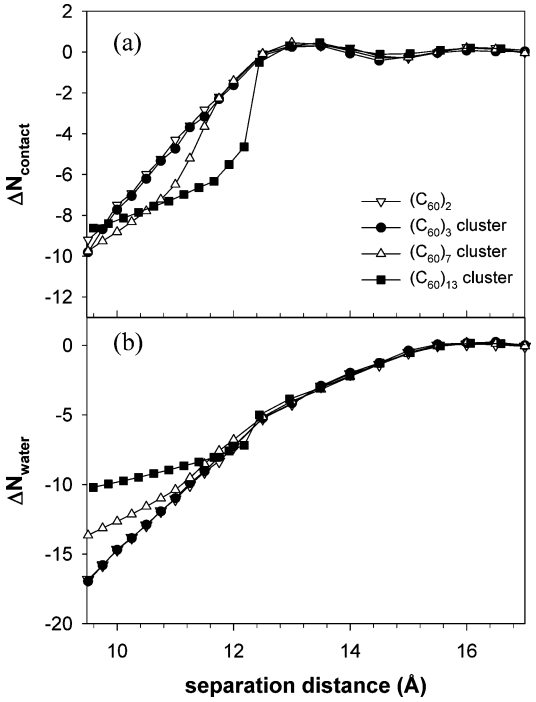

Figure 5. The change in the number of (a) water-fullerene contacts (see text) and (b) hydrating water molecules for each cluster as a function of fullerene separation, normalized by the number of nearest neighbor fullerene pairs.

the presence of the third fullerene does not perturb the interaction between the (two) nearest neighbor pairs. For the planar $(C_{60})_7$ cluster, the fully atomistic simulation predicts a slightly stronger attractive interaction between fullerenes at the close contact position but no discernible difference from the two-body prediction for separations greater than about 11 Å. In contrast, significant differences in the PMF can be seen between the two-body prediction and the atomistic simulations for the 3-dimensional $(C_{60})_{13}$ cluster, indicating that pair interactions are strongly perturbed by the presence of other fullerenes (i.e., the existence of many-body effects). The primary minimum is significantly deeper and broader than predicted by the two-body potential, indicating that many-body effects promote fullerene−fullerene attraction at short separation.

C. Water-Induced Interactions. The PMF for the fullerene clusters in vacuum was determined using a Brownian dynamics integrator and the same constraint protocol described above for the clusters in aqueous solution. The (normalized per nearest neighbor pair) PMF in vacuo is shown in Figure 4a. The in vacuo PMF for all clusters is described nearly perfectly by the two-body (pair) PMF, implying that any dependence of the free energy of formation of clusters in water on cluster geometry is due to differences in water-induced interactions.

Figure 4b shows the water-induced contribution to the PMF for each cluster, obtained by subtracting the in vacuo PMF from the PMF obtained in aqueous solution. We first note that the water-induced contribution is a minor component of the total PMF for all clusters (compare to the total PMF in Figure 2), indicating that fullerene−fullerene interactions are dominated by direct van der Waals interactions and not by solvent effects. For all cluster geometries the influence of water on fullerene interaction is repulsive, i.e., water leads to a positive contribution to the free energy of pair formation for all separations, as discussed in our previous work[1,2] and in the Introduction to this paper for $(C_{60})_2$.

In Figure 5a the number of water-fullerene contacts for all cluster geometries, normalized by the number of nearest neighbor pairs, is shown as a function of separation relative to that for large separation. In other words, Figure 5a shows the change in the number of water-fullerene contacts as the separation between fullerenes decreases from large separation. A water-fullerene contact is considered to exist whenever a water molecule is within the first hydration shell of fullerene, i.e., within 8.38 Å of the center of the fullerene.[1] Figure 5b shows the change in the number of hydrating water molecules as a function of separation, again normalized by the number of nearest neighbor pairs. For all cluster geometries the number of contacts is almost constant down to a separation of about 12−12.5 Å, at which point the single layer of hydrating water between the fullerenes (which has contact with two or more fullerenes) begins to be squeezed out and the number of water contacts drops with decreasing separation. In contrast, the number of hydrating water begins to decrease at separations around 15 Å when the second layer of hydrating water starts to be squeezed out and fullerenes begin to share hydrating water molecules.

Figure 4b reveals that the water-induced contribution to the PMF for the fullerene pair $(C_{60})_2$ has maxima at

separations of around 11 Å and 14.5 Å. At these separations, neither a single hydration layer nor two hydration layers, respectively, can be well accommodated between the fullerenes, while the minima at 13 Å and 16 Å correspond to distances that can accommodate the hydrating water structure well. The water-induced contribution to the free energy of formation for the $(C_{60})_3$ cluster is nearly identical to that for the fullerene pair, reflecting the fact that in the linear geometry the shell fullerenes are too far removed from each other to significantly influence hydration of the shell-central fullerene pairs. The similarity in behavior for the linear cluster and $(C_{60})_2$ pair is further emphasized in Figure 5, where a nearly identical smooth loss of water contacts and hydrating water is observed with decreasing separation.

For the close-packed planar geometry, $(C_{60})_7$, Figure 4b reveals some influence of geometry on the water-induced contribution to the free energy of formation. The maximum in the water-induced contribution to the free energy is shifted slightly to larger separations compared to the fullerene pair and linear cluster, and the unfavorable contribution of water to the free energy of cluster formation drops rapidly with decreasing separation for separations less than 11.5 Å. This difference in behavior of the water-induced contribution to the free energy of formation for the 1-dimensional and 2-dimensional clusters is reflected in a greater loss in the number of water-fullerene contacts for the $(C_{60})_7$ cluster (per nearest neighbor pair) and a loss of fewer hydrating water molecules (per nearest neighbor pair) than is observed for the linear geometry for separations less than about 11.5 Å. At this separation the water within the interior of the cluster (as opposed to those water molecules hydrating the exterior surface of the aggregate) becomes unstable, and these relatively constrained, high free energy water molecules, which interact simultaneously with multiple fullerenes and hence form several water-fullerene contacts, are rapidly expelled from the cluster with decreasing separation.

Continued release of constrained water molecules on the surface of the $(C_{60})_7$ cluster with decreasing separation (similar to the effect observed for the pair and linear aggregate) for separations less than about 11.5 Å accounts for the decrease in the unfavorable water-induced contribution to the free energy of formation with decreasing separation. This can be thought of as an interfacial effect. Water interacts favorably with isolated fullerenes. As the fullerenes are brought together, relatively high free energy water is created that must interact with multiple fullerenes. The cluster reaches a maximum free energy at the point where the constrained water in the interior to the cluster is the most frustrated. Further decrease in separation results in release of this water. However, constrained water (water interacting with multiple fullerenes) also exists on the surface of the cluster which is only released gradually as the surface area of the cluster decreases, accounting for the decrease in the unfavorable water induced interaction with decreasing separation.

The effect of many-body interactions on the water-induced contribution to the free energy of cluster formation is more dramatic for the 3-dimensional geometry, as can be clearly seen in Figure 4b. The maximum unfavorable contribution of water is shifted to a significantly larger separation, and the magnitude of the maximum decreases dramatically compared to the 1- and 2-dimensional clusters. This difference is reflected in a dramatic drop in the number of water-fullerene contacts and number of hydrating water at separations of around 12 Å as shown in Figure 5. As revealed by Figure 6, which shows the number of water molecules involved with hydrating the central fullerene, this dramatic drop in the number of water-fullerene contacts results from the complete dehydration of the central fullerene. As with the 1-dimensional and 2-dimensional clusters, decrease in the water-induced contribution to the free energy of formation for separations less than 12 Å reflects the continued release of highly constrained water hydrating the exterior surface of the cluster. We anticipate that the latter effect becomes weaker as the size of the 3-dimensional cluster increases and interfacial effects become less important compared to the effects in the cluster interior.

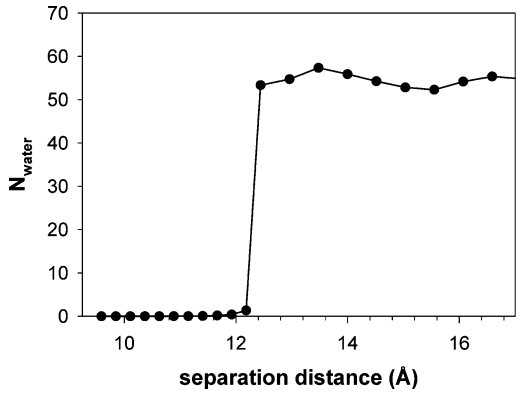

Figure 6. The number of water molecules hydrating the central fullerene in the $(C_{60})_{13}$ cluster as a function of fullerene separation.

IV. Conclusions

In summary, our investigation of the influence of geometry on the free energy of formation of C_{60} clusters in aqueous solution reveals that direct fullerene−fullerene interactions dominate over water induced interactions for all dimensionalities. The water-induced repulsion observed for a single fullerene pair is found to weaken with increasing cluster dimension, particularly for the 3-dimensional (icosahedral) cluster. This weakening of the water-induced repulsion reflects the importance of many-body interactions for the more compact geometries, i.e., the important role of neighboring fullerenes on the water-induced interaction between any pair of fullerenes. We believe the reduction in the water-induced repulsion for the 3-dimensional aggregate is due to both the creation of fewer highly constrained, high free energy water molecules, i.e., water solvating more than one fullerene, compared to 1-dimensional and 2-dimensional aggregates, and the overall loss of fewer hydrating water (per contact pair) than is predicted based upon the behavior of a single fullerene pair. Both effects result from the overlap of hydration shells of multiple fullerenes in the compact 3-dimensional geometry.

Acknowledgment. The authors gratefully acknowledge support from the National Science Foundation through grants NSF ITR CHE0312226 and MRSEC (University of Colorado) DMR-0213918.

References

(1) Li, L.; Bedrov, D.; Smith, G. D. *Phys. Rev. E* **2005**, *71*, 011502.

(2) Li, L.; Bedrov, D.; Smith, G. D. *J. Chem. Phys.* **2005**, *123*, 204504.

(3) Slanina, Z.; Pulay, P.; Nagase, S. *J. Chem. Theory Comput.* **2006**, *2*, 782−785.

(4) Bedrov, D.; Smith, G. D.; Li, L. *Langmuir* **2005**, *21*, 5251−5255.

(5) Gallego, L. J.; Garcia-Rodeja, J.; Alemany, M. M. G.; Rey, C. *Phys. Rev. Lett.* **1999**, *83*, 5258−5261.

(6) Piatek, A.; Dawid, A.; Gburski, Z. *J. Phys.: Condens. Matter* **2006**, *18*, 8471−8480.

(7) http://www.che.utah.edu/~gdsmith/mdcode/main.html (accessed Aug 5, 2005).

(8) Allen, M. P.; Tildesley, D. J. Building the model potential. In *Computer Simulation of Liquids*; Oxford University Press; Clarendon, Oxford, 1989; p 9.

(9) Jorgensen, W. L.; Chandrasekhar, J.; Madura, J. D.; Impey, R. W.; Klei, M. *J. Chem. Phys.* **1983**, *79*, 926−935.

(10) Werder, T.; Walther, J. H.; Jaffe, R. L.; Halicioglu, T.; Koumoutsakos, P. *J. Phys. Chem. B* **2003**, *107*, 1345−1352.

(11) Ryckaert, J. P.; Ciccotti, G.; Berendsen, H. J. C. *J. Comput. Phys.* **1977**, *23*, 327−341.

(12) Essmann, U.; Perera, L.; Berkowitz, M. L.; Darden, T.; Lee, H.; Pedersen, L. G. *J. Chem. Phys.* **1995**, *103*, 8577−8593.

(13) Tuckerman, M.; Berne, B. J.; Martyna, G. L. *J. Chem. Phys.* **1991**, *94*, 6811−6815.

(14) Tuckerman, M.; Berne, B. J.; Martyna, G. L. *J. Chem. Phys.* **1992**, *97*, 1990−2001.

CT700211Y